NEURO

Karsten Papke
Friedhelm Brassel

Modern cross-sectional imaging in the diagnosis and follow-up of intracranial aneurysms

K. Papke (✉) · F. Brassel
Department of Radiology and
Neuroradiology, Klinikum Duisburg,
Zu den Rehwiesen 9,
47055 Duisburg, Germany
e-mail: karsten.papke@klinikum-
duisburg.de
Tel.: +49-203-7332700
Fax: +49-203-7332702

Abstract Digital subtraction angiography (DSA) is still considered the gold standard for most applications in neurovascular imaging. However, with the ongoing development of cross-sectional imaging modalities DSA is increasingly being replaced by less invasive methods. This contribution describes the diagnostic value and the increasing potential of computed tomography angiography (CTA) and magnetic resonance angiography (MRA) in the diagnosis and follow-up of intracranial aneurysms. The main role of CTA is in the diagnosis and therapy planning of ruptured aneurysms; in contrast, MRA plays an increasingly important role in the screening for asymptomatic aneurysms (especially in cases of familial subarachnoid hemorrhage) and in the follow-up after endovascular therapy with coils and/or intracranial stents. Technical issues concerning examination technique are covered here as well as an approach to advanced postprocessing of the image data. Furthermore, a brief outlook on the impact of new developments (MRA with parallel imaging and at 3.0 T) is given.

Keywords M Magnetic resonance angiography · Intracranial aneurysm · Multidetector computed tomography angiography

Introduction

With the ongoing advances in cross-sectional imaging the noninvasive imaging of vascular disorders has reached unprecedented quality. In computed tomography angiography both the spatial and temporal resolution have been greatly increased by the development of multidetector CTA (MDCTA). Magnetic resonance angiography (MRA) has been stimulated by faster gradient systems, parallel imaging techniques, and increased static magnetic field.

Neurovascular imaging is particularly challenging due to the small size of functionally relevant vascular structures and due to the short arteriovenous transit time in the cerebrovascular circulation, which may even be shortened by neurovascular disorders such as arteriovenous malformations. Therefore both high-spatial and high-temporal resolution are required for diagnostic image quality. As this combination of prerequisites is best achieved with intra-arterial digital subtraction angiography (DSA), this method is still considered the standard of reference for most neurovascular imaging applications. However, with their recent advances, cross-sectional imaging modalities continue to grow as a complement to or even replacement for DSA in neurovascular imaging [1]. Paralleling the progress of CT and MRI, advanced postprocessing algorithms such as three-dimensional (3D) isosurface display and volume rendering technique have developed from a sophisticated toy to a working tool that is more readily available on modern CT and MR consoles or on separate workstations for clinical routine use. Given the complex 3D shape of neurovascular structures it is now acknowledged that appropriate postprocessing strategies improves the diagnostic performance of CT and MRI.

This contribution illustrates the role of modern cross-sectional imaging in the diagnosis and therapy planning of intracranial aneurysms and their follow-up after therapy.

Magnetic resonance angiography imaging techniques

Time-of-flight magnetic resonance angiography

3D time-of-flight (TOF) MRA is the MRI technique most often used to depict intracranial arteries. The vessel contrast in TOF MRA is based on the inflow effect: stationary tissue is suppressed by repetitive radiofrequency pulses while unsaturated protons entering the imaging volume with the flowing blood yield high signal intensity. Relevant limitations of 3D TOF MRA are signal loss in turbulent flow and the high signal intensity of stationary tissues with short T1 such as fat or subacute thrombus (methemoglobin). Furthermore, signal loss especially in small distal vessels may occur due to spin saturation. Saturation effects may be reduced by a technique called "multiple overlapping thin slab acquisition" and by the variable flip-angle excitation technique termed "tilted optimized nonsaturating excitation" [2]. In addition, magnetization transfer contrast may be applied to improve small-vessel depiction [3, 4], alone or in combination with intravenous administration of Gd-DTPA [5, 6].

As a more recent alternative to fat suppression, spectral-spatial water excitation may be used to suppress high signal caused by fat [7, 8]. In intracranial vessels water excitation allows better background suppression than conventional (i.e., magnetization transfer contrast saturated) 3D TOF acquisitions especially in the orbits and at the periphery [6]. However, one must be aware that water excitation may produce artifacts mimicking stenosis or occlusion of the carotid artery [9].

Phase-contrast magnetic resonance angiography

Phase-contrast (PC) MRA is another flow-dependent imaging technique which is, however, only rarely used for depiction of intracranial arteries [10]. 3D PC MRA is very time consuming because four acquisitions are required to encode flow in all directions. With respect to the detection of intracranial aneurysms 3D PC MRA is significantly inferior to 3D TOF MRA [11, 12]. Therefore 3D PC MRA is not discussed further here.

Contrast-enhanced magnetic resonance angiography

Contrast-enhanced (ce) MRA during the first-pass of a contrast bolus continues to be developed as a complementary technique to study the intracranial vasculature. Unlike 3D TOF MRA, it requires a gradient system with high slew rates for ultrafast acquisitions and additional tools for the proper timing of the scan with respect to the bolus arrival [13]. Due to the short arteriovenous transition time in the cerebral circulation, early enhancement of venous structures limits the time window for scan acquisition, and a

trade-off is therefore necessary between scan time, volume coverage and spatial resolution [14]. Subtraction of an unenhanced data set from the contrast enhanced data set may be performed to suppress residual high signal of nonvascular structures [15].

Parallel imaging

Parallel acquisition techniques (PAT) have recently been developed and are now being increasingly used for vascular imaging. PAT uses multichannel coil arrays to shorten the measurement time by reducing the number of phase encoding steps. The spatial information is instead extracted from the sensitivity profiles of the coil elements. Numerous image acquisition algorithms have been described, including SENSE (sensitivity encoding), SMASH (simultaneous acquisition of spatial harmonics), and GRAPPA (generalized autocalibrating partially parallel acquisitions) [16–18].

In intracranial 3D TOF imaging PAT with an eight-channel phased-array head coil has been used to save 43% of measurement time while maintaining the same image quality [6]. However, it must be kept in mind that using PAT reduces the signal-to-noise ratio (SNR) by approximately the square root of the acceleration factor [19]. The inherently high SNR of contrast enhanced MRI makes PAT particularly suited for ceMRA.

In arterial ceMRA PAT can be used to accelerate the acquisition (and hence avoid venous contamination), to increase spatial resolution and/or volume coverage, or to combine the two [19].

Intracranial magnetic resonance angiography at 3.0 T

Recent studies have evaluated the advantages of higher magnetic field strength (3.0 T). It has been demonstrated that vessel-to-background contrast is superior with 3.0 T to that with 1.5 T [20]. The increased SNR obtained with TOF MRA at 3.0 T makes it possible to increase the spatial resolution; using a high-resolution 3D TOF MRA protocol at 3.0 T with a voxel size of 0.30×0.44×1.00 mm, the image quality and the depiction of small vessel segments have been found superior to standard resolution at 1.5 and 3.0 T [21].

Computed tomography angiography imaging technique

The introduction of MDCTA has helped overcome some inherent limitations of single-slice CTA for the diagnosis of intracranial aneurysms because it allows faster imaging of larger volumes with increased spatial resolution. In single-slice CTA the limited acquisition volume in z-direction has been a notorious cause of missing aneurysms (e.g., periclosal aneurysms cephalad or posterior inferior cerebellar

artery aneurysms caudad to the scan volume) [22, 23]. Furthermore, given the short arteriovenous transition time of only a few seconds, aneurysms within the cavernous sinus or close to other venous structures may be obscured by venous enhancement. In contrast, with MDCTA and precise timing of the contrast bolus, arterial and venous structures become distinguishable owing to their different attenuation during the short acquisition phase for the entire imaging volume. This holds particularly true for 16-row MDCTA with a typical scan duration of 5 s for the intracranial arteries.

At our institution we use 16-row MDCTA (Siemens Somatom Sensation 16) with a collimation of 16×0.75 mm, rotation time of 0.5 s, and table feed of 11.0 mm/rotation. Images are reconstructed with a slice thickness of 1.0 mm and an increment of 0.8 mm. For assessment of aneurysm morphology the reconstruction kernel should not be too soft because the aneurysm neck may appear too wide and lobulations of an aneurysm may be obscured; we use a slightly edge enhancing kernel (H45f).

A total volume of 50 ml (for 16-row MDCTA) of an iodine-based contrast medium (300 mg iodine/ml) is injected at a flow rate of 4 ml/s, followed by a chaser bolus of 20 ml NaCl 0.9%. Bolus arrival is observed with a monitoring scan at the level of C4, and spiral scanning is started manually with a delay of 2 s as soon as the contrast bolus arrives in the carotid arteries.

Screening for unruptured aneurysms

The estimated prevalence of intracranial aneurysms in Western countries is 2.3% as calculated from a meta-analysis based on more than 56,000 patients. With the development and increasing distribution of MRA aneurysms are being detected more frequently as asymptomatic incidental findings [24]. However, the annual rate of bleeding from incidental aneurysms is very low. Depending on the size of the aneurysm 5-year cumulative rupture rates between 2.6% (7–12 mm diameter) and 50% (>25 mm diameter) have been calculated [25]. To assess the potential benefit of screening for unruptured aneurysms the risk from aneurysmal rupture must be compared with the risk of therapy. The procedural morbidity and mortality of endovascular aneurysm treatment are 3.7% and 1%, respectively [26]. Although this risk is considerably lower than the risk of neurosurgical clipping with a morbidity and mortality of 10.9% and 2.6% [27], the relationship between rupture risk and risk of aneurysm treatment does not justify a systematic screening for asymptomatic aneurysms in healthy individuals.

On the other hand, familial clustering of aneurysms is observed in approx. 10% of patients with subarachnoid hemorrhage (SAH) [28, 29]. Aneurysms in so-called familial SAH (defined as two or more first-degree relatives known to have SAH or unruptured aneurysms) tend to rupture earlier in life and at smaller size [30]. Therefore a repeated screening for aneurysms in this patient group has

been recommended [31–33]. The benefit of repeated screening for aneurysms in familial SAH has been confirmed [34]. In this study MRA was performed in patients without prior therapy of aneurysms while CTA was used if neurosurgical clipping had been applied in the past. The authors reported a high yield of repeated screening. However, the period during which screening should be repeated is not yet certain. A period of 5 years appears to be too long in some cases to detect all new familial aneurysms [34]. Concerning the modality to be chosen for familial screening, the high examination frequency required to detect all de novo aneurysms favors MRA over CTA except in patient after neurosurgical clipping. The use of MRA is also supported by the fact that there is no significant difference in the diagnostic performance between MRA and CTA [35].

Aneurysm detection with intracranial magnetic resonance angiography

The detection rates for intracranial aneurysm using MRA vary with aneurysm size. A study using 3D TOF MRA with a matrix size of 512×256 reported an aneurysm diameter of 5 mm as the critical size for detection [11]. More recent studies have been shown 3D TOF MRA to identify aneurysms larger than 3 mm with a sensitivity between 74% and 98% [36–38]. Comparing ceMRA and 3D TOF MRA in a series of 23 aneurysms, a sensitivity of 100% has been reported for ceMRA compared to 96% for 3D TOF MRA; however, this difference was not statistically significant [12]. Therefore it has been concluded that the detection rates for intracranial aneurysms do not differ significantly between ceMRA and 3D TOF MRA [10].

When assessing the diagnostic value of MRA for intracranial aneurysm screening, one must keep in mind that the size dependence of the detection sensitivity constitutes an important limitation. Although the risk of aneurysmal rupture increases with aneurysm size, even very small aneurysms (2 mm or less) may rupture [37], and if they do so, they even have a tendency to provoke larger bleedings [39].

On the other hand, DSA as the gold standard for aneurysm detection is not an alternative to noninvasive screening with MRA, owing to its invasiveness; therefore it remains desirable that the ongoing technical progress of MRA will translate into a higher sensitivity in the detection of small aneurysms. It may be expected that the SNR with MRA at 3.0 T can improve the sensitivity to detect small aneurysms, and TOF MRA at 3.0 T has been confirmed as superior to a 1.5-T TOF technique for characterizing intracranial aneurysms [40]. A comparison of TOF MRA and ceMRA at 3.0 T reported that TOF MRA provided better image quality and a higher sensitivity for aneurysm detection [41].

At our institution we use a standard 3D TOF technique with tilted optimized nonsaturating excitation, magnetiza-

tion transfer contrast saturation, and water excitation at 1.5 T with TR/TE=40 ms/4.97 ms and a flip angle of 25° (Siemens Magnetom Sonata). Three or four overlapping thin-slabs are acquired with an effective voxel size of 0.9×0.4×1.0 mm. To distinguish between flow related hyperintensity and hyperintensity of structures with short T1 (e.g., methemoglobin in a thrombus) it may be helpful to acquire an additional data set with arterial presaturation. Remaining bright signal can then be identified as non-flow-related, and the arterially presaturated data set can be subtracted from the original data set with bright vascular signal. In the subtracted data set all remaining hyperintensity is flow related (Fig. 1).

Therapy planning of intracranial aneurysms with magnetic resonance angiography

In addition to the detection of intracranial aneurysms, MRA has also been used to characterize aneurysm morphology with the intention to assess the suitability for coil embolization. TOF MRA has been found to be inferior to DSA in the pretreatment assessment of intracranial aneurysms, but it can provide complementary information to DSA [42]. In a different study, however, Atlas et al. [43] reported that TOF MRA is inadequate for the characterization of aneurysms. These findings are consistent with our own experience. To our opinion, the main limitation of TOF MRA in the assessment of aneurysm morphology is the fact that high signal represents flow rather than the real boundaries of the aneurysm. At TOF MRA slow flow within the aneurysm may escape detection and provide false impression of aneurysm morphology; furthermore, signal inhomogenieties due, for example, to spin dephasing may lead to an imprecise depiction of the aneurysm neck. We therefore do not rely on TOF MRA alone for therapy planning but perform an additional ceMRA if an aneurysm is detected at TOF MRA (Fig. 2).

For intracranial ceMRA we use a 3D fast low-angle shot sequence with TR/TE=3.68/1.37 ms. Eighty partitions 0.8 mm thick are acquired within 21 s with an effective voxel size of 0.9×0.7×0.8 mm. The standard head coil is used in combination with a neck coil and the segment coils in the patient table. The field of view is chosen to cover the upper part of the aortic arch up to the circle of Willis. A bolus of 20 ml Gd-DTPA is administered at a flow rate of 2 ml/s, followed by a saline flush with the same volume and flow rate. Bolus timing is achieved with a coronal single

Fig. 1 Diagnostic value of 3D TOF MRA with arterial saturation subtraction. Large fusiform dissecting aneurysm of the basilar artery. **a**, **b** Axial source image of 3D TOF MRA, with venous saturation (**a**) and arterial saturation (**b**). Crescent-shaped hyperintensity in the dorsolateral aspect of the aneurysm which persists with arterial saturation, consistent with intramural thrombus. **c** VRT display of a subtracted data set (3D TOF with venous saturation minus 3D TOF with arterial saturation to eliminate the high signal of the thrombus) demonstrates the impression of the lumen by the thrombus and makes it possible to appreciate the three-dimensional shape of the perfused lumen. **d** DSA of the aneurysm
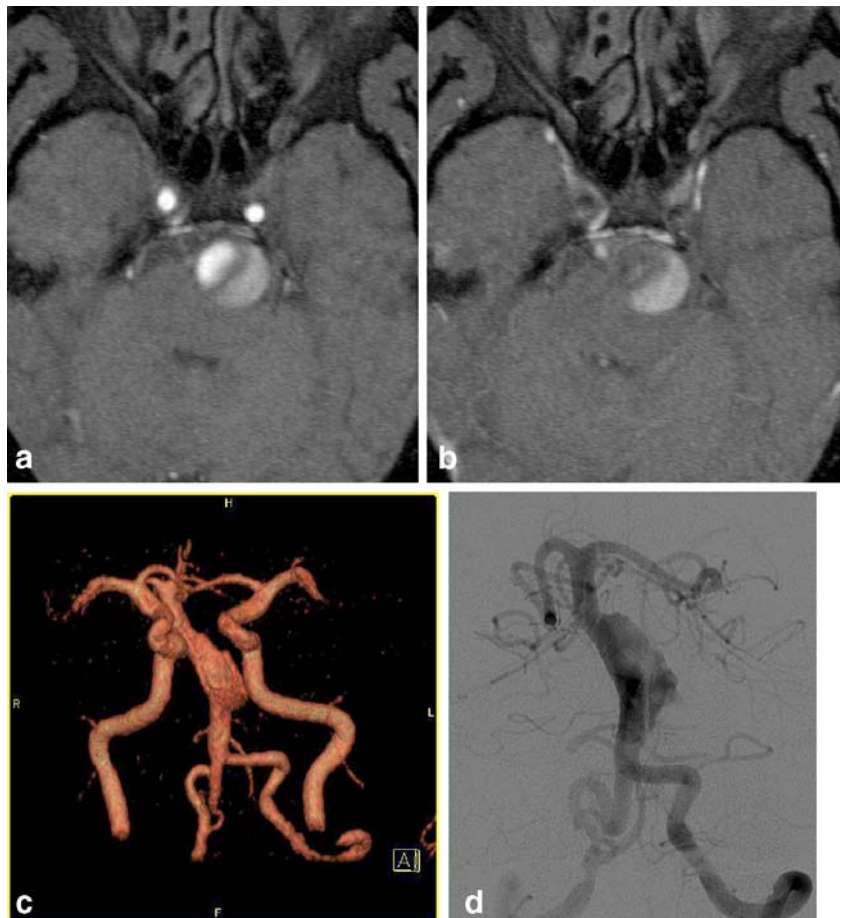
Fig. 2 Incidental aneurysm in the supraophthalmic segment of the right inferior cerebellar artery. **a, b** Parasagittal thin-slab MIP of 3D TOF MRA (**a**) and contrast-enhanced MRA (**b**), both with identical slab thickness (50 mm) and projection angle. Note that both the aneurysm lumen and the neck are depicted more sharply in ceMRA. **c** The VRT display of the ceMRA data set provides depth information about the topographic relationship between the aneurysm and adjacent vessels. Based on the results of MRA it was anticipated that the aneurysm could be treated with coil embolization. **d** DSA performed immediately before successful coil embolization confirms the findings of MRA
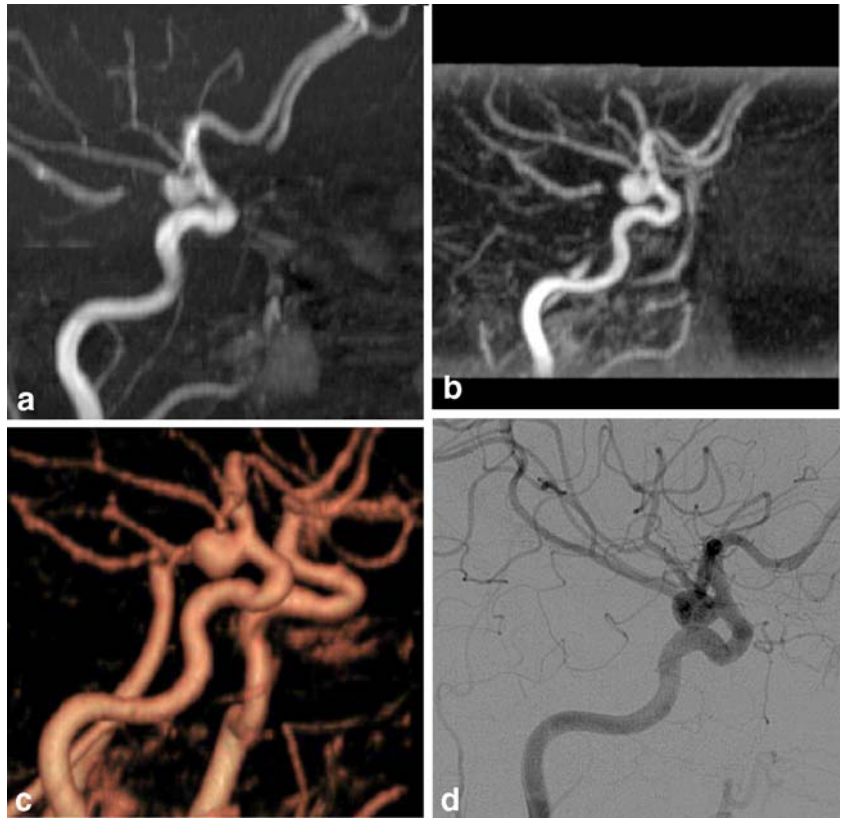
thick-slice (40 mm) monitoring scan. The 3D acquisition is started manually as soon as the contrast bolus is seen to start entering the intracranial carotid arteries. Due to centric k-space filling the contrast-sensitive central parts of the k-space are filled during the first seconds of the acquisition.

Precontrast images are obtained for image subtraction to obtain a better suppression of nonvascular background signal. A transverse orientation is chosen for better spatial coverage of the intracranial arteries as compared to the coronal orientation. A disadvantage of the transverse orientation is given by the fact that the high inflow signal of the carotid and vertebral arteries in the precontrast images leads to signal loss in the subtracted images. Therefore unsubtracted postcontrast images must be analyzed in addition to the subtracted images.

Postprocessing

Maximum intensity projection (MIP) is the postprocessing algorithm most widely used for the display of MRA data sets. MIP is a projection technique in which only the brightest voxels of a volume are collected and used to create an image [44]. It is important to note that postprocessing with MIP entails a reduction in image information to about 10% of the full source images [45]. A further limitation of MIP is that it is not per se a 3D technique but a projection of a 3D data volume into a two-dimensional plane. This means

that MIP images do not contain any depth information, and the relationship of aneurysms to their parent vessels and other adjacent vascular structures cannot be directly extracted from MIP images. It has therefore been criticized that despite these known limitations, most MRA studies dealing with detection of intracranial aneurysms have relied on MIP postprocessing of the image data [42].

Numerous studies have emphasized the diagnostic value of advanced surface-based postprocessing techniques such as an isosurface algorithm [42] or a multifeature-extraction, ray-tracing algorithm [43]. It has been reported that volume rendering provides more reliable detection and better characterization of aneurysms than MIP postprocessing [46]. However, despite all modern postprocessing techniques it is still essential to refer to the axial source images in addition, because only these images contain the full information and are not subject to artifacts introduced by the respective postprocessing technique [47].

For standardized postprocessing and for a first inspection we obtain MIP of the entire data set in angulated projections (11 images in sagittal to coronal to sagittal orientation and 7 in transverse to coronal orientation). In addition, an interactive analysis of the data set is performed, including inspection of the source images and angulated thin-slab MIP in appropriate projections to inspect typical aneurysm locations. To obtain true 3D images a direct volume-rendering of the data set with interactive real-time rotation is carried out on a separate workstation. Positive findings are

documented and stored in representative projections. Furthermore, axial source images of positive findings are stored.

Diagnosis and treatment planning in ruptured aneurysms

In acutely ruptured aneurysms, the role of imaging is (a) to demonstrate the presence, extent and distribution of hemorrhage, (b) to identify the source of bleeding (i.e., the ruptured aneurysm), (c) to provide a pre-treatment assessment of the detected aneurysm with the intention to decide whether coil embolization or neurosurgical clipping is the preferred therapy, and (d) to rule out additional unruptured aneurysms [48]. The latter aspect is important because patients with more than one intracranial aneurysm carry an increased risk of aneurysmal rupture after SAH from the first aneurysm ranging from 0.5% to 2.4% per year [49].

In the emergency setting of acute subarachnoid hemorrhage CT is the imaging modality of first choice in most institutions because MRI and MRA is often impractical in severely affected patients [50]. Unenhanced cranial CT to demonstrate subarachnoid hemorrhage may be combined with intracranial CTA in the same session. Therefore MRA has only rarely been reported in the management of acutely ruptured aneurysms [42, 51]. In contrast, many studies have demonstrated the value of CTA and raise the question to the extent to which CTA might replace DSA in the workup of intracranial aneurysms. Being an invasive diagnostic procedure, DSA carries an additional risk of morbidity and mortality both by the procedure itself [52, 53] and by the fact that effective treatment may be delayed, especially if diagnostic DSA and occlusion of the aneurysm are performed at different institutions.

Aneurysm detection with computed tomography angiography

Since the first reports on intracranial CTA using single-slice CTA [54–60,] this noninvasive technique has been playing an increasingly important role in SAH. A systematic review calculated a diagnostic accuracy of 89% per aneurysm for CTA using single-slice technique [61]. Another meta-analysis with weighted calculations for the number of patients in each study reported a weighted sensitivity and specificity of 92.7% and 77.2% [23]. Detection rates vary with aneurysm size [61, 62]. A study using four-row MDCTA, a reader-dependent sensitivity of 81–90% was observed with a specificity of 93%; all aneurysms that were missed in this study were identified retrospectively after correlation with DSA [63]. In our own series of 81 patients examined with 4- and 16-row MDCTA the overall sensitivity for aneurysm detection was 96%;

even small aneurysms with a diameter of 3 mm or less were recognized with a sensitivity of 85% (Fig. 3).

Treatment planning

Concerning presurgical therapy planning for intracranial aneurysms numerous studies have emphasized the value of CTA [64–67], and several groups rely on CTA as the sole preoperative imaging modality prior to neurosurgical clipping of intracranial aneurysms. Concerning the planning of endovascular treatment 26 aneurysms were considered suitable for endovascular coil embolization on single-slice CTA in a study of 123 patients, but DSA demonstrated contraindications in 5 patients [66]. The appropriate diameter of the first detachable coil was correctly chosen in six of seven patients based on CTA measurements [68].

In our own experience with 74 potentially ruptured aneurysms examined by 16-row MDCTA 47 aneurysm were correctly classified as suitable for coil embolization and 22 correctly identified as not suitable for coil embolization, resulting in a positive predictive value (PPV) of 96% and a negative predictive value (NPV) of 88%. This assessment was based on the estimation of neck width in relation to aneurysm size and on the presence of vessels originating from the aneurysm with a risk of occlusion by the coils; an aneurysm was defined as suited for coil embolization if coils could be placed in the aneurysm without supportive techniques such as balloon remodeling or stent placement. Based on this experience we rely on MDCTA results to decide whether an aneurysm is suited for coil embolization without additional diagnostic DSA (Fig. 4). This is particularly important in patients referred to us from other institutions. However, it is important in such cases that the source images are available for own postprocessing.

Postprocessing

As in MRA, the diagnostic quality of CTA is also affected by postprocessing [50]. The MIP algorithm is also frequently used for the display of CT angiographic data. However, in CTA the MIP algorithm is limited by the higher density of bone than the opacified vessels. This means that whenever a vessel and bone are situated on the same projection beam, the vessel is masked by the bone. It has therefore been concluded that postprocessed images should always be compared carefully with the axial source images [47]. Given the nearly isotropic nature of MDCTA data sets monitoring of the axial source images can be supplemented by interactive multiplanar reformats in order to detect aneurysms at locations that are not well depicted in the axial plane.

At our institution the axial source images are inspected first. Each vascular segment is then inspected interactively using thin-slice (1 mm) multiplanar reformats and thin-slab MIP (5–8 mm) using the 3D tool of the workstation. This

Fig. 3 Small intracranial aneurysm, directed medially from the paraophthalmic portion of the right inferior cerebellar artery. **a** CTA (para-axial MIP, slab thickness 10 mm). **b** ceMRA (para-axial MIP, slab thickness 10 mm). Despite the small size both CTA and ceMRA demonstrate the aneurysm which is only barely visible with DSA (**c**)
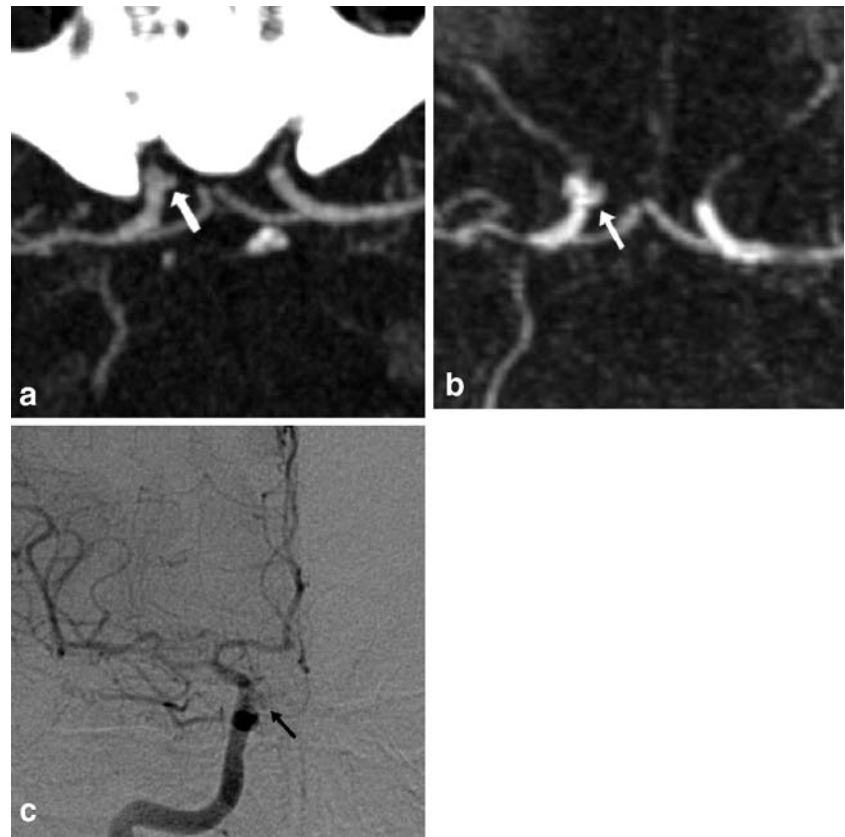
analysis includes inspection of the data in the axial orientation and in two more orientations that are chosen parallel and orthogonal to the main course of the respective vascular segment. For the picture archiving and communication system thin-slab MIPs are created (8 mm slab thickness with 3 mm increment) in axial, sagittal, and paracoronal orientation (parallel to the clivus). Representative volume rendering technique (VRT) and MIP images of positive findings with appropriate slab thickness and orientation are stored in addition. The axial source images are also stored in a CD archive for future reference.

As it has been demonstrated for MRA that VRT provides better visualization of intracranial aneurysms than does the MIP algorithm [46], we routinely use interactive VRT display in addition. To identify possible working projections prior to endovascular therapy of an aneurysm the data set is rotated interactively so that the aneurysm and the parent vessel become visible in one plane without superimposing vascular structures. The VRT preset is then changed to a transparent bone display. This image is stored and sent to the angio suite, where it is used to position the C-arm to the same projection angle (Fig. 4). Given the variety of postprocessing algorithms described above, it has been correctly reported that there are as yet no standardized and reproducible methods for 3D visualiza-tion available, and it is emphasized that studies performed so far evaluate specific systems, and the results depend on the experience of individual users [45].

Follow-up after therapy of intracranial aneurysms

Although there are no general recommendations on time periods, frequency, or imaging methods, it is widely accepted that patients who undergo treatment of an intracranial aneurysm require follow-up by neurovascular imaging [69–73]. This is based on the fact that: (a) de novo aneurysms may develop after successful treatment of the initial aneurysm and (b) complete occlusion of the aneurysm needs to be verified and might not be permanent (e.g., due to aneurysm regrowth or reperfusion). For follow-up of intracranial aneurysms after therapy the choice of the adequate imaging modality is influenced and limited by the applied form of treatment. Following neurosurgical clipping, MRA is impossible due to susceptibility artifacts caused by the clip material. On the other hand, following endovascular coiling the high radiodensity of platinum coils precludes useful CTA examinations owing to the severe beam hardening artifacts.

Fig. 4 Therapy planning for an aneurysm of the anterior communicating artery with MDCTA. **a** MDCTA with VRT display of the aneurysm showing the size of the aneurysm, its neck, and its relationship to the parent vessels. Based on MDCTA, the decision to perform endovascular treatment was made. With interactive rotation of the volume rendered CTA data set, an adequate working projection for the subsequent endovascular therapy has been identified. **b** Using this projection angle, the MDCTA data set is presented as a projectionlike image by changing the VRT density transfer function. This image is presented in the angio suite and is used to adjust the C-arm to the same working projection under fluoroscopic control. **c** DSA before coil embolization and **d** after coil embolization of the aneurysm
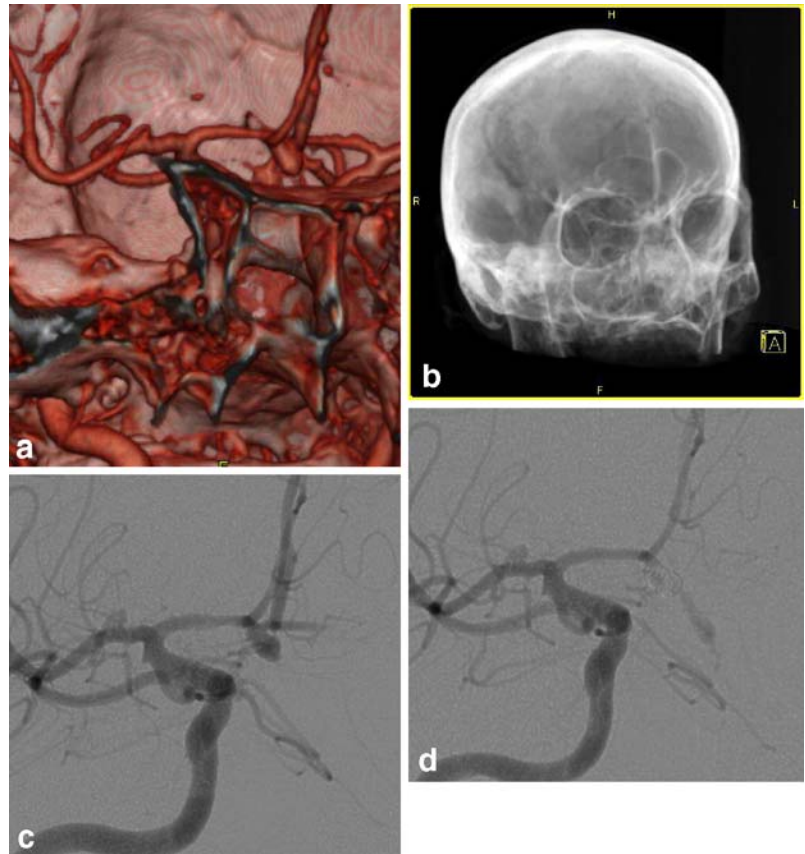
Follow-up after neurosurgical clipping

Most studies concerning follow-up of neurosurgically clipped aneurysms have used DSA for imaging [69, 70, 74]. After a mean follow-up period of 9 years regrowth of a clipped aneurysm was found to have occurred in 2.9%, whereas de novo aneurysms had formed in 8.0% [70]. To our knowledge, there are no generally accepted recommendations on the follow-up of clipped aneurysms. In most cases the decision to verify the success of surgery by means of imaging is therefore made on an individual basis, based on such factors as the confidence of the neurosurgeon in correct clip positioning and anatomical difficulty.

MRA is not an alternative to DSA for the follow-up of clipped intracranial aneurysms; although vascular clips made of titanium or titanium alloy are MRI-safe even at 3.0 T [75], their susceptibility artifacts with signal voids surrounding the clip interfere with MRA [76, 77]. Therefore CTA is the only less invasive imaging modality that might replace DSA. It has been claimed that CTA may be used for postoperative evaluation of aneurysms especially when titanium clips were used [76–78]. On the other hand, it has been demonstrated that beam hardening artifacts may mimic occlusion of nearby vessel even with MDCTA, and it has been concluded that MDCTA is of little value for the follow-up of clipped aneurysms in most cases [45]. However, CTA

with a tilted head positioning has been proposed to avoid interference of beam hardening artifacts with adjacent vessels of interest [79]. To our limited own experience, CTA after clipping of intracranial aneurysms is sometimes helpful if the beam hardening artifacts do not interfere with the display of vessels adjacent to the clip (Fig. 5). We think that the preliminary results are promising enough to warrant further studies.

Follow-up after coil embolization

Embolization of intracranial aneurysms via the endovascular route was first described in 1991 [80, 81]. Within a decade endovascular coiling had gained widespread acceptance as an alternative to neurosurgical clipping. Short-term results of endovascular clipping have now been demonstrated to be superior to neurosurgical clipping in aneurysms in which both kinds of treatment are therapeutic options [82]. However, recanalization occurs in approx. 20% of coiled aneurysms especially after incomplete coiling [83], due either to aneurysm regrowth or to compaction of the coil package with an associated risk of rebleeding [26]. Therefore angiographic follow-up has been found mandatory after aneurysm embolization [83], and it has been recommended to perform DSA 3 months, 1 year, and 3 years after treatment [84]. Due

Fig. 5 Sixteen-row MDCTA before (**a**) and immediately after (**b**) neurosurgical clipping of a trifurcation aneurysm of the right MCA. **c**, **d** In thin-slab (10 mm) MIP (**c**) and in the axial source images (**d**) the titanium clip produces only minor beam hardening artifacts. Even the patency of vessels in the vicinity of the clip can be assessed
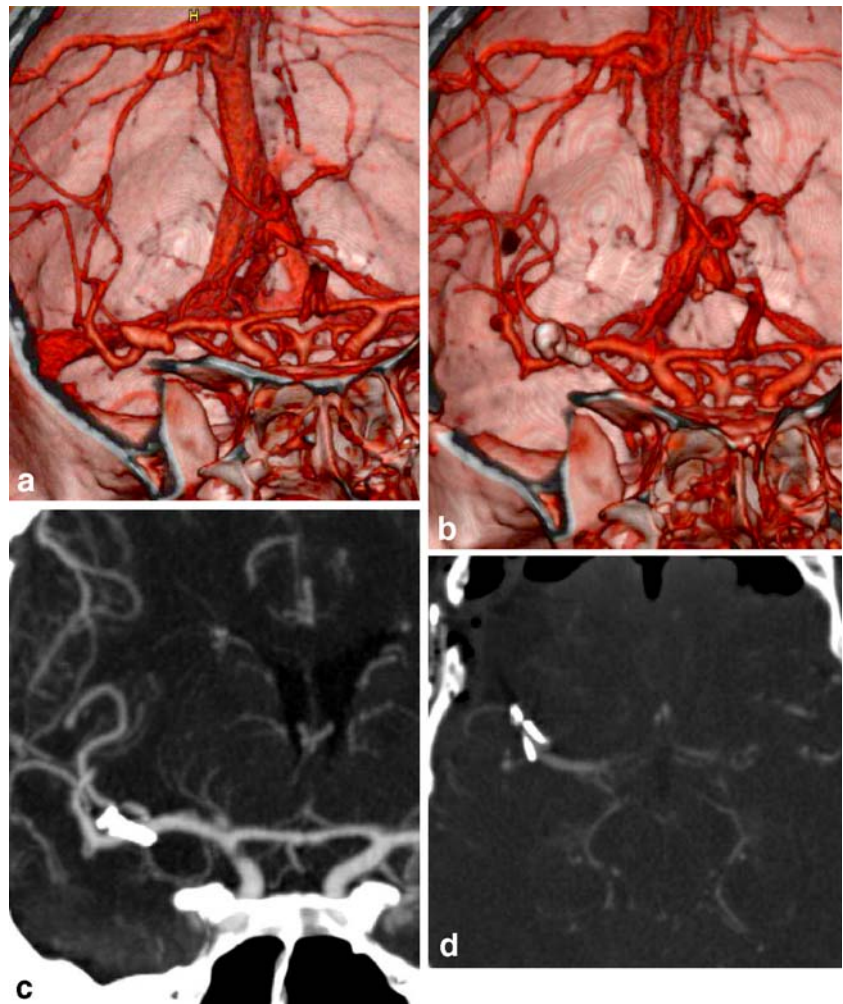
to the invasiveness of DSA with a 1% major complication risk and a 0.5% rate of persistent neurological deficit [53], MRA has been studied as an alternative for follow-up of coiled intracranial aneurysms.

Three-dimensional time-of-flight magnetic resonance angiography

Platinum coils are MRI safe [85] and have been found to produce only minor artifacts even at 3.0 T [86]. Derdeyn et al. [87] correctly identified the patency of the parent artery with a sensitivity of 96%; residual flow in the aneurysms was detected with a sensitivity and specificity of 71% and 89%, respectively. Brunereau et al. [88] reported a sensitivity of 83% and a specificity of 100% to diagnose residual flow within the aneurysmal neck with 3D TOF MRA. The high sensitivity of 3D TOF MRA in the detection of aneurysmal recurrence has been confirmed in further studies [89–92].

Comparisons of MRA and DSA have emphasized that flow within the coil package may be depicted even better with MRA than with DSA [90]. Compared to 3D DSA, a sensitivity of 72.7% and a specificity 90.9% has been reported for the diagnosis of residual or recurrent aneurysm [93]. A recent study even claimed targeted 3D TOF MRA with ultrafast TE to be superior to DSA in the detection of residual flow in the aneurysm [94].

False-negative findings at 3D TOF MRA may be caused by slow flow in the aneurysm leading to saturation [87], turbulent flow creating intravoxel dephasing [88], or magnetic susceptibility artifacts of the coil package creating a signal void [93, 95]. False-positive results were related to the presence of high-signal rim artifacts around the coil package [87] or intra- or extraluminal blood clot interpreted as flow at MRA [85]. Coil-induced signal voids may furthermore present as pseudoencroachment of arteries adjacent to the coil package [89]. It has been reported that the depiction of vessels adjacent to the coil package can be improved with MRA using ultra-short TE [96]; however, later study did not

confirm an improvement in image quality using a similar ultra-fast technique [90]. The additional use of contrast material in 3D TOF imaging does not improve visualization of residual aneurysms except in large aneurysms where compartments with slow flow may be better visualized after contrast administration [90, 92].

Despite these limitations most authors agree that after primary concurrent demonstration of equal results with 3D TOF MRA and DSA, MRA is suited for further follow-up of coiled aneurysms [89–91, 94]. With respect to the follow-up scheme proposed by Cognard et al. [84], it has been proposed to replace the 3 months follow-up study by MRA and perform both DSA and MRA after 1 year. If equal results are demonstrated, the future follow-up can then be based on MRA [91, 94].

Contrast enhanced first-pass magnetic resonance angiography)

More recently the value of ceMRA for follow-up of coiled aneurysms was examined, and in three incompletely occluded aneurysms the visualization of residual perfusion was better with ceMRA than with 3D TOF MRA [14]. These results were subsequently confirmed in a larger series of 29 coiled aneurysms. The sensitivity and specificity in detecting residual aneurysm components was 81% and 88% with ceMRA and 40% and 90% with 3D TOF MRA [97]. In the 6-month follow-up of 48 intracranial aneurysms with ceMRA sensitivity and specificity values of 100% and 92% were found for the detection of a residual neck or aneurysm [98].

Fig. 6 Reperfusion of an aneurysm at the origin of the left MCA following coil embolization. **a, b** 3D TOF MRA (**a**) and ceMRA (**b**) both displayed as thin-slab MIP (4 mm). The conspicuousness is higher, and the demonstrated extent of reperfusion is larger with ceMRA. **c, d** VRT display of ceMRA (**c**) and of rotational 3D DSA (**d**) in a similar projection, demonstrating two compartments of reperfusion at the base and at the dorsal circumference of the coiled aneurysm. **e, f** DSA before (**e**) and after (**f**) stent placement and coil embolization of the aneurysm remnant
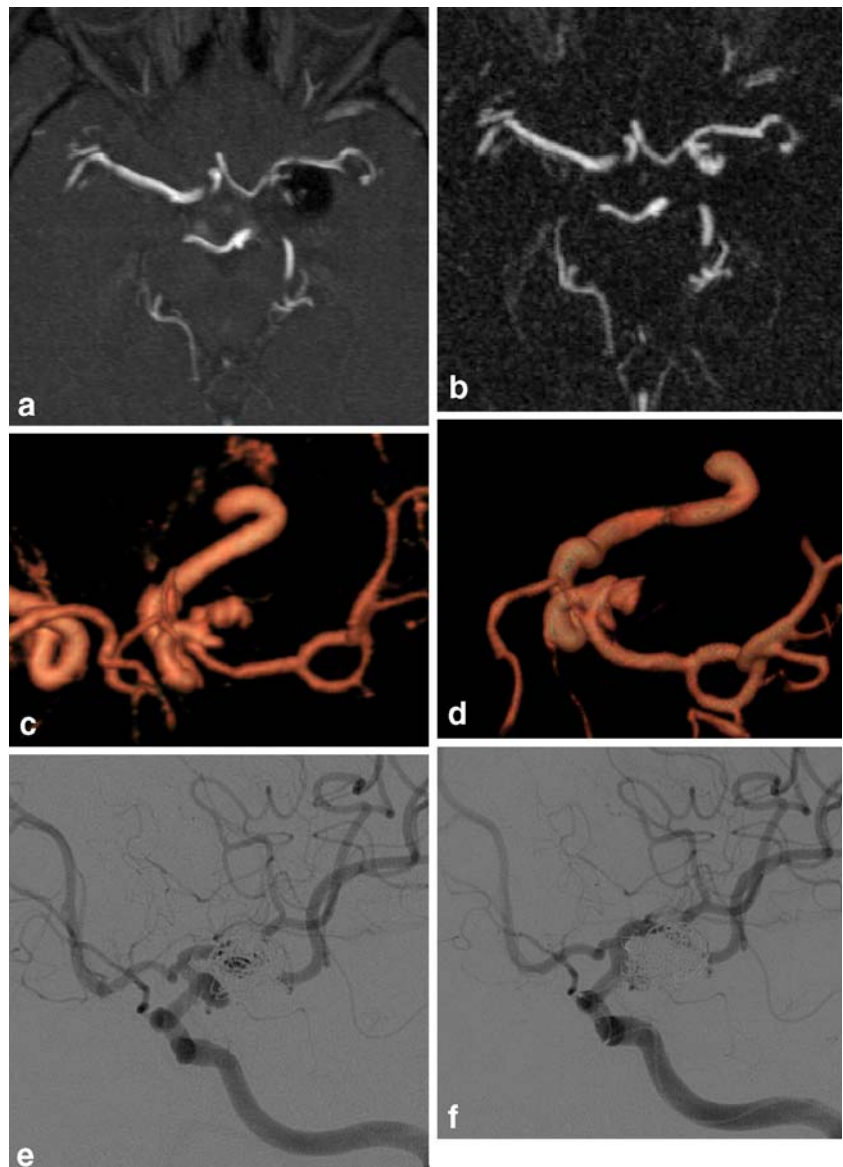
At our institution we use 3D TOF MRA and ceMRA to compliment one another in the follow-up of aneurysms after coil embolization. In direct comparison the conspicuousness for residual aneurysms is higher with ceMRA, and their extent is depicted more precisely (Fig. 6). On the other hand, small parent vessels such as the posterior communicating artery may be better delineated by 3D TOF than by ceMRA due to the higher spatial resolution. Furthermore, ceMRA sometimes suffers from venous contamination interfering with identification of de novo aneurysms. However, careful interpretation of axial or coronal source images of ceMRA

may provide accurate information about the residual aneurysm and its relations with adjacent vascular structures, even in the case of venous contamination.

Follow-up after stenting, stent-protected coil embolization, and embolization with onyx

The initial applications of stents in combination with coils to treat intracranial aneurysms in humans were described in 1998 [99–102]. For stent-assisted coil embolization a stent

Fig. 7 Residual perfusion at the base of a distal inferior cerebellar artery aneurysm, status following stent protected coil embolization. **a** DSA demonstrating the residual aneurysm measuring approx. 2 mm. **b**, **c** The residual lesion was followed up with 3D TOF (**b**) and ceMRA (**c**); both examinations are displayed as thin-slab MIP with identical slab thickness of 30 mm. The lesion is visible only with ceMRA. **d**, **e** Also in the axial source images, the lesion is not identified in 3D TOF MRA (**d**), whereas it is clearly depicted in ceMRA (**e**)

is placed in the parent vessel so that it covers the orifice of the aneurysm before a microcatheter is advanced into the aneurysm through the stent struts. When filling the aneurysm with coils, protrusion of the coils into the vessel lumen may be prevented by the stent even in wide-necked aneuryms. Stent placement alone without subsequent coiling may also be a therapeutic option [103], especially in dissecting and/or fusiform aneurysms. Metallic stents originally developed for cardiological applications have been used in these cases. More recently a self-expanding, microcatheter-delivered nitinol stent dedicated to intracranial use has been introduced and has been used in larger series of intracranial aneurysms [104–106]. Another recent endovascular technique for aneurysm treatment is embolization with a liquid polymer (Onyx) which is dissolved in dimethylsulfoxide. Onyx is used especially in wide-necked large and giant aneurysms [107, 108], either in combination with a balloon remodeling technique or with additional stent placement.

Concerning imaging follow-up after intravascular stenting there is ongoing controversy regarding the role of MRA [109]. In phantom studies using Gd-enhanced MRA the depiction of the stent lumen ranged from good visualization to complete signal void throughout the lumen, depending on the stent type [109, 110]. Therefore when using MRA for follow-up after stent implantation, one must be aware of the MR properties of the particular stent type used.

With particular reference to the first dedicated intracranial self-expanding stent (Neuroform, Boston Scientific), it has been stated that MRI with this stent is safe and feasible even at 3 T [111]. Patients treated with this stent have been followed up with 3D TOF MRA; no relevant stent-related artifacts have been reported [105], and the patency of the parent vessel and emerging branches has been assessable [104, 106]. However, in our experience, small residual aneurysms may escape detection with 3D TOF MRA alone. Therefore we recommend adding ceMRA to 3D TOF MRA in the follow-up after stent protected coil embolization of cerebral aneurysms (Fig. 7). If stenting of a fusiform aneurysm is performed without subsequent coil deployment, CTA may be an alternative to demonstrate stent patency or to identify stent thrombosis. Concerning embolization with Onyx, it has been demonstrated that this liquid embolic material does not interfere with MRA except when combined with a stent, whereas severe beam hardening artifacts occur with CT [112].

Conclusion

Due to the ongoing development of cross-sectional imaging DSA as the gold standard for neurovascular imaging is gradually replaced by MDCTA and MRA in the diagnosis and follow-up of intracranial aneurysms. MDCTA is a valuable tool for detection of intracranial aneurysms in the acute setting of subarachnoid hemorrhage; the decision as to whether an aneurysm is suited for coil embolization can usually be based on MDCTA alone without an additional diagnostic DSA. Furthermore, the 3D information of MDCTA can be used to support endovascular treatment planning by assessing aneurysm morphology, by the relationship to the parent vessels, and by finding a suited working projection. Concerning neurosurgical clipping, an increasing number of neurosurgeons rely on CTA as the sole preoperative imaging. The role of MDCTA for follow-up after neurosurgical clipping remains to be defined; follow-up after endovascular coil embolization is impossible with MDCTA due to artifacts of the coil package.

3D TOF MRA is particularly suited for screening for intracranial aneurysms due to its noninvasiveness and the capability to reliably identify aneurysms larger than 3 mm. Furthermore, it is frequently used for follow-up after coil embolization and has a high diagnostic precision in identifying aneurysmal remnants. Aneurysms that have been treated with recent self-expanding microcatheter delivered intracranial stents can also be examined with 3D TOF MRA. Contrast-enhanced MRA, if available, should be used to complement 3D TOF MRA in the follow-up of endovascularly treated aneurysms because aneurysm remnants may be identified with higher sensitivity, and their morphology is depicted more precisely.

References

1. Anzalone N, Scomazzoni F, Strada L, Patay Z, Scotti G (1998) Intracranial vascular malformations. Eur Radiol 8:685–690

2. Atkinson D, Brant-Zawadzki M, Gillan G, Purdy D, Laub G (1994) Improved MR angiography: magnetization transfer suppression with variable flip angle excitation and increased resolution. Radiology 190:890–894

3. Edelman RR, Ahn SS, Chien D, Li W, Goldmann A, Mantello M, Kramer J, Kleefield J (1992) Improved time-of-flight MR angiography of the brain with magnetization transfer contrast. Radiology 184:395–399

4. Pike GB, Hu BS, Glover GH, Enzmann DR (1992) Magnetization transfer time-of-flight magnetic resonance angiography. Magn Reson Med 25:372–379

5. Mathews VP, Ulmer JL, White ML, Hamilton CA, Reboussen DM, Elster AD (1999) Depiction of intracranial vessels with MRA: utility of magnetization transfer saturation and gadolinium. J Comput Assist Tomogr 23:597–602

6. Özsarlak O, Van Goethem JW, Parizel PM (2004) 3D time-of-flight MR angiography of the intracranial vessels: optimization of the technique with water excitation, parallel acquisition, eight-channel phased-array head coil and low-dose contrast administration. Eur Radiol 14:2067–2071

7. Schick F (1996) Pulsed magnetization transfer contrast MRI by a sequence with water selective excitation. J Comput Assist Tomogr 20:73–79

8. Hatabu H, Gaa J, Stock KW, Li W, Thomasson D, Edelman RR (1999) Application of a spectral-spatial water excitation for MR angiography. Eur J Radiol 29:253–258

9. Gizewski ER, Ladd ME, Paul A, Wanke I, Goricke S, Forsting M (2005) Water excitation: a possible pitfall in cerebral time-of-flight angiography. Am J Neuroradiol 26:152–155

10. Özsarlak O, Van Goethem JW, Maes M, Parizel PM (2004) MR angiography of the intracranial vessels: technical aspects and clinical applications. Neuroradiology 46:955–972

11. Huston J, III, Nichols DA, Luetmer PH, Goodwin JT, Meyer FB, Wiebers DO, Weaver AL (1994) Blinded prospective evaluation of sensitivity of MR angiography to known intracranial aneurysms: importance of aneurysm size. Am J Neuroradiol 15:1607–1614

12. Metens T, Rio F, Baleriaux D, Roger T, David P, Rodesch G (2000) Intracranial aneurysms: detection with gadolinium-enhanced dynamic three-dimensional MR angiography-initial results. Radiology 216:39–46

13. Bosmans H, Wilms G, Dymarkowski S, Marchal G (2001) Basic principles of MRA. Eur J Radiol 38:2–9

14. Gottschalk S, Gaebel C, Haendler G, Gellissen J, Missler U, Seidel G, Nowak G, Petersen D (2002) Contrast-enhanced intracranial 3 D MR angiography (CE-MRA) in assessing arterial stenoses and aneurysms (in German). Rofo Fortschr Geb Rontgenstr Neuen Bildgeb Verfahr 174:704–713

15. Lee VS, Flyer MA, Weinreb JC, Krinsky GA, Rofsky NM (1996) Image subtraction in gadolinium-enhanced MR imaging. Am J Roentgenol 167:1427–1432

16. Pruessmann KP, Weiger M, Scheidegger MB, Boesiger P (1999) SENSE: sensitivity encoding for fast MRI. Magn Reson Med 42:952–962

17. Sodickson DK, McKenzie CA, Ohliger MA, Yeh EN, Price MD (2002) Recent advances in image reconstruction, coil sensitivity calibration, and coil array design for SMASH and generalized parallel MRI. MAGMA 13:158–163

18. Griswold MA, Jakob PM, Heidemann RM, Nittka M, Jellus V, Wang J, Kiefer B, Haase A (2002) Generalized auto-calibrating partially parallel acquisitions (GRAPPA). Magn Reson Med 47:1202–1210

19. Heidemann RM, Ozsarlak O, Parizel PM, Michiels J, Kiefer B, Jellus V, Muller M, Breuer F, Blaimer M, Griswold MA, Jakob PM (2003) A brief review of parallel magnetic resonance imaging. Eur Radiol 13:2323–2337

20. Al-Kwifi O, Emery DJ, Wilman AH (2002) Vessel contrast at three tesla in time-of-flight magnetic resonance angiography of the intracranial and carotid arteries. Magn Reson Imaging 20:181–187

21. Willinek WA, Born M, Simon B, Tschampa HJ, Krautmacher C, Gieseke J, Urbach H, Textor HJ, Schild HH (2003) Time-of-flight MR angiography: comparison of 3.0-T imaging and 1.5-T imaging-initial experience. Radiology 229:913–920

22. Ohkawa M, Tanabe M, Toyama Y, Kimura N, Mino S, Takayama K, Satoh G (1998) CT angiography with helical CT in the assessment of acute stage of subarachnoid hemorrhage. Radiat Med 16:91–97

23. Chappell ET, Moure FC, Good MC (2003) Comparison of computed tomographic angiography with digital subtraction angiography in the diagnosis of cerebral aneurysms: a meta-analysis. Neurosurgery 52:624–631

24. Wilms G, Demaerel P, Bosmans H, Marchal G (1999) MRI of non-ischemic vascular disease: aneurysms and vascular malformations. Eur Radiol 9:1055–1060

25. Wiebers DO, Whisnant JP, Huston J, III, Meissner I, Brown RD Jr, Piepgras DG, Forbes GS, Thielen K, Nichols D, O'Fallon WM, Peacock J, Jaeger L, Kassell NF, Kongable-Beckman GL, Torner JC (2003) Unruptured intracranial aneurysms: natural history, clinical outcome, and risks of surgical and endovascular treatment. Lancet 362:103–110

26. Brilstra EH, Rinkel GJ, van der Graaf Y, van Rooij WJ, Algra A (1999) Treatment of intracranial aneurysms by embolization with coils: a systematic review. Stroke 30:470–476

27. Raaymakers TW, Rinkel GJ, Limburg M, Algra A (1998) Mortality and morbidity of surgery for unruptured intracranial aneurysms: a meta-analysis. Stroke 29:1531–1538

28. Schievink WI (1997) Genetics of intracranial aneurysms. Neurosurgery 40:651–662

29. van Gijn J, Rinkel GJ (2001) Subarachnoid haemorrhage: diagnosis, causes and management. Brain 124:249–278

30. Ronkainen A, Hernesniemi J, Tromp G (1995) Special features of familial intracranial aneurysms: report of 215 familial aneurysms. Neurosurgery 37:43–46

31. Raaymakers TW, Rinkel GJ, Ramos LM (1998) Initial and follow-up screening for aneurysms in families with familial subarachnoid hemorrhage. Neurology 51:1125–1130

32. Bederson JB, Awad IA, Wiebers DO, Piepgras D, Haley EC Jr, Brott T, Hademenos G, Chyatte D, Rosenwasser R, Caroselli C (2000) Recommendations for the management of patients with unruptured intracranial aneurysms: a statement for healthcare professionals from the Stroke Council of the American Heart Association. Stroke 31:2742–2750

33. Brown BM, Soldevilla F (1999) MR angiography and surgery for unruptured familial intracranial aneurysms in persons with a family history of cerebral aneurysms. Am J Roentgenol 173:133–138

34. Wermer MJ, Rinkel GJ, van Gijn J (2003) Repeated screening for intracranial aneurysms in familial subarachnoid hemorrhage. Stroke 34:2788–2791

35. White PM, Teasdale EM, Wardlaw JM, Easton V (2001) Intracranial aneurysms: CT angiography and MR angiography for detection prospective blinded comparison in a large patient cohort. Radiology 219:739–749

36. Bosmans H, Wilms G, Marchal G, Demaerel P, Baert AL (1995) Characterisation of intracranial aneurysms with MR angiography. Neuroradiology 37:262–266

37. Chung TS, Joo JY, Lee SK, Chien D, Laub G (1999) Evaluation of cerebral aneurysms with high-resolution MR angiography using a section-interpolation technique: correlation with digital subtraction angiography. Am J Neuroradiol 20:229–235

38. White PM, Wardlaw JM, Lindsay KW, Sloss S, Patel DK, Teasdale EM (2003) The non-invasive detection of intracranial aneurysms: are neuroradiologists any better than other observers? Eur Radiol 13:389–396

40. Gibbs GF, Huston J III, Bernstein MA, Riederer SJ, Brown RD Jr (2004) Improved image quality of intracranial aneurysms: 3.0-T versus 1.5-T time-of-flight MR angiography. Am J Neuroradiol 25:84–87

41. Gibbs GF, Huston J III, Bernstein MA, Riederer SJ, Brown RD Jr (2005) 3.0-Tesla MR angiography of intracranial aneurysms: comparison of time-of-flight and contrast-enhanced techniques. J Magn Reson Imaging 21:97–102

42. Adams WM, Laitt RD, Jackson A (2000) The role of MR angiography in the pretreatment assessment of intracranial aneurysms: a comparative study. Am J Neuroradiol 21:1618–1628

43. Atlas SW, Sheppard L, Goldberg HI, Hurst RW, Listerud J, Flamm E (1997) Intracranial aneurysms: detection and characterization with MR angiography with use of an advanced postprocessing technique in a blinded-reader study. Radiology 203:807–814

44. Prokop M, Shin HO, Schanz A, Schaefer-Prokop CM (1997) Use of maximum intensity projections in CT angiography: a basic review. Radiographics 17:433–451

45. Tomandl BF, Kostner NC, Schempershofe M, Huk WJ, Strauss C, Anker L, Hastreiter P (2004) CT angiography of intracranial aneurysms: a focus on postprocessing. Radiographics 24:637–655

46. Mallouhi A, Felber S, Chemelli A, Dessl A, Auer A, Schocke M, Jaschke WR, Waldenberger P (2003) Detection and characterization of intracranial aneurysms with MR angiography: comparison of volume-rendering and maximum-intensity-projection algorithms. Am J Roentgenol 180:55–64

47. Velthuis BK, van Leeuwen MS, Witkamp TD, Boomstra S, Ramos LM, Rinkel GJ (1997) CT angiography: source images and postprocessing techniques in the detection of cerebral aneurysms. Am J Roentgenol 169:1411–1417

48. U-King-Im JM, Koo B, Trivedi RA, Higgins NJ, Tay KY, Cross JJ, Antoun NM, Gillard JH (2005) Current diagnostic approaches to subarachnoid haemorrhage. Eur Radiol 15:1135–1147

49. Wanke I, Egelhof T, Dorfler A, Forsting M (2003) Intracranial aneurysms: pathogenesis, rupture risk, treatment options (in German). Rofo Fortschr Geb Rontgenstr Neuen Bildgeb Verfahr 175:1064–1070

50. Gasparotti R, Liserre R (2005) Intracranial aneurysms. Eur Radiol 15:441–447

51. Sankhla SK, Gunawardena WJ, Coutinho CM, Jones AP, Keogh AJ (1996) Magnetic resonance angiography in the management of aneurysmal subarachnoid haemorrhage: a study of 51 cases. Neuroradiology 38:724–729

52. Cloft HJ, Joseph GJ, Dion JE (1999) Risk of cerebral angiography in patients with subarachnoid hemorrhage, cerebral aneurysm, and arteriovenous malformation: a meta-analysis. Stroke 30:317–320

53. Heiserman JE, Dean BL, Hodak JA, Flom RA, Bird CR, Drayer BP, Fram EK (1994) Neurologic complications of cerebral angiography. Am J Neuroradiol 15:1401–1407

54. Aoki S, Sasaki Y, Machida T, Ohkubo T, Minami M (1992) Cerebral aneurysms: detection and delineation using 3-D-CT angiography. Am J Neuroradiol 13:1115–1120

55. Alberico RA, Ozsvath R, Casey S, Patel M (1996) Helical CT angiography for the detection of intracranial aneurysms. Am J Neuroradiol 17:1002–1003

56. Alberico RA, Patel M, Casey S, Jacobs B, Maguire W, Decker R (1995) Evaluation of the circle of Willis with three-dimensional CT angiography in patients with suspected intracranial aneurysms. Am J Neuroradiol 16:1571–1578

57. Harbaugh RE, Schlusselberg DS, Jeffery R, Hayden S, Cromwell LD, Pluta D (1992) Three-dimensional computerized tomography angiography in the diagnosis of cerebro vascular disease. J Neurosurg 76:408–414

58. Dorsch NW, Young N, Kingston RJ, Compton JS (1995) Early experience with spiral CT in the diagnosis of intracranial aneurysms. Neurosurgery 36:230–236

59. Brown JH, Lustrin ES, Lev MH, Ogilvy CS, Taveras JM (1997) Characterization of intracranial aneurysms using CT angiography. Am J Roentgenol 169:889–893

60. Anderson GB, Findlay JM, Steinke DE, Ashforth R (1997) Experience with computed tomographic angiography for the detection of intracranial aneurysms in the setting of acute subarachnoid hemorrhage. Neurosurgery 41:522–527

61. White PM, Wardlaw JM, Easton V (2000) Can noninvasive imaging accurately depict intracranial aneurysms? A systematic review. Radiology 217:361–370

62. van Gelder JM (2003) Computed tomographic angiography for detecting cerebral aneurysms: implications of aneurysm size distribution for the sensitivity, specificity, and likelihood ratios. Neurosurgery 53:597–605

63. Jayaraman MV, Mayo-Smith WW, Tung GA, Haas RA, Rogg JM, Mehta NR, Doberstein CE (2004) Detection of intracranial aneurysms: multi-detector row CT angiography compared with DSA. Radiology 230:510–518

64. Anderson GB, Steinke DE, Petruk KC, Ashforth R, Findlay JM (1999) Computed tomographic angiography versus digital subtraction angiography for the diagnosis and early treatment of ruptured intracranial aneurysms. Neurosurgery 45:1315–1320

65. Boet R, Poon WS, Lam JM, Yu SC (2003) The surgical treatment of intracranial aneurysms based on computer tomographic angiography alone-streamlining the acute mananagement of symptomatic aneurysms. Acta Neurochir (Wien) 145:101–105

66. Dehdashti AR, Rufenacht DA, Delavelle J, Reverdin A, de Tribolet N (2003) Therapeutic decision and management of aneurysmal subarachnoid haemorrhage based on computed tomographic angiography. Br J Neurosurg 17:46–53

67. Zouaoui A, Sahel M, Marro B, Clemenceau S, Dargent N, Bitar A, Faillot T, Capelle L, Marsault C (1997) Three-dimensional computed tomographic angiography in detection of cerebral aneurysms in acute subarachnoid hemorrhage. Neurosurgery 41:125–130

68. Jansen O, Braks E, Hahnel S, Schramm T, Sartor K (1998) [CT angiography to determine the size of intracranial aneurysms before GDC therapy]. Rofo Fortschr Geb Rontgenstr Neuen Bildgeb Verfahr 169:175–181

69. Thornton J, Bashir Q, Aletich VA, Debrun GM, Ausman JI, Charbel FT (2000) What percentage of surgically clipped intracranial aneurysms have residual necks? Neurosurgery 46:1294–1298

70. Tsutsumi K, Ueki K, Morita A, Usui M, Kirino T (2001) Risk of aneurysm recurrence in patients with clipped cerebral aneurysms: results of long-term follow-up angiography. Stroke 32:1191–1194

71. Thornton J, Debrun GM, Aletich VA, Bashir Q, Charbel FT, Ausman J (2002) Follow-up angiography of intracranial aneurysms treated with endovascular placement of Guglielmi detachable coils. Neurosurgery 50:239–249

72. Matheus MG, Castillo M (2003) Development of de novo intracranial aneurysm in three months: case report and literature review. Am J Neuroradiol 24:709–710

73. Akyuz M, Tuncer R, Yilmaz S, Sindel T (2004) Angiographic follow-up after surgical treatment of intracranial aneurysms. Acta Neurochir (Wien) 146:245–250

74. Sindou M, Acevedo JC, Turjman F (1998) Aneurysmal remnants after microsurgical clipping: classification and results from a prospective angiographic study (in a consecutive series of 305 operated intracranial aneurysms). Acta Neurochir (Wien) 140:1153–1159

75. Shellock FG, Tkach JA, Ruggieri PM, Masaryk TJ, Rasmussen PA (2003) Aneurysm clips: evaluation of magnetic field interactions and translational attraction by use of "long-bore" and "short-bore" 3.0-T MR imaging systems. Am J Neuroradiol 24: 463–471

76. van Loon JJ, Yousry TA, Fink U, Seelos KC, Reulen HJ, Steiger HJ (1997) Postoperative spiral computed tomography and magnetic resonance angiography after aneurysm clipping with titanium clips. Neurosurgery 41:851–856

77. Steiger HJ, van Loon JJ (1999) Virtues and drawbacks of titanium alloy aneurysm clips. Acta Neurochir Suppl 72:81–88

78. Kato Y, Nair S, Sano H, Sanjaykumar MS, Katada K, Hayakawa M, Kanno T (2002) Multi-slice 3D-CTA-an improvement over single slice helical CTA for cerebral aneurysms. Acta Neurochir (Wien) 144:715–722

79. Brown JH, Lustrin ES, Lev MH, Ogilvy CS, Taveras JM (1999) Reduction of aneurysm clip artifacts on CT angiograms: a technical note. Am J Neuroradiol 20:694–696

80. Guglielmi G, Vinuela F, Sepetka I, Macellari V (1991) Electrothrombosis of saccular aneurysms via endovascular approach. I. Electrochemical basis, technique, and experimental results. J Neurosurg 75:1–7

81. Guglielmi G, Vinuela F, Dion J, Duckwiler G (1991) Electrothrombosis of saccular aneurysms via endovascular approach. II. Preliminary clinical experience. J Neurosurg 75:8–14

82. Molyneux A, Kerr R, Stratton I, Sandercock P, Clarke M, Shrimpton J, Holman R (2002) International Subarachnoid Aneurysm Trial (ISAT) of neurosurgical clipping versus endovascular coiling in 2143 patients with ruptured intracranial aneurysms: a randomised trial. Lancet 360:1267–1274

83. Murayama Y, Nien YL, Duckwiler G, Gobin YP, Jahan R, Frazee J, Martin N, Vinuela F (2003) Guglielmi detachable coil embolization of cerebral aneurysms: 11 years' experience. J Neurosurg 98:959–966

84. Cognard C, Weill A, Spelle L, Piotin M, Castaings L, Rey A, Moret J (1999) Long-term angiographic follow-up of 169 intracranial berry aneurysms occluded with detachable coils. Radiology 212:348–356

85. Shellock FG, Detrick MS, Brant-Zawadski MN (1997) MR compatibility of Guglielmi detachable coils. Radiology 203:568–570

86. Shellock FG, Gounis M, Wakhloo A (2005) Detachable coil for cerebral aneurysms: in vitro evaluation of magnetic field interactions, heating, and artifacts at 3T. Am J Neuroradiol 26:363–366

87. Derdeyn CP, Graves VB, Turski PA, Masaryk AM, Strother CM (1997) MR angiography of saccular aneurysms after treatment with Guglielmi detachable coils: preliminary experience. Am J Neuroradiol 18:279–286

88. Brunereau L, Cottier JP, Sonier CB, Medioni B, Bertrand P, Rouleau P, Sirinelli D, Herbreteau D (1999) Prospective evaluation of time-of-flight MR angiography in the follow-up of intracranial saccular aneurysms treated with Guglielmi detachable coils. J Comput Assist Tomogr 23:216–223

89. Kähärä VJ, Seppanen SK, Ryymin PS, Mattila P, Kuurne T, Laasonen EM (1999) MR angiography with three-dimensional time-of-flight and targeted maximum-intensity-projection reconstructions in the follow-up of intracranial aneurysms embolized with Guglielmi detachable coils. Am J Neuroradiol 20:1470–1475

90. Anzalone N, Righi C, Simionato F, Scomazzoni F, Pagani G, Calori G, Santino P, Scotti G (2000) Three-dimensional time-of-flight MR angiography in the evaluation of intracranial aneurysms treated with Guglielmi detachable coils. Am J Neuroradiol 21:746–752

91. Boulin A, Pierot L (2001) Follow-up of intracranial aneurysms treated with detachable coils: comparison of gadolinium-enhanced 3D time-of-flight MR angiography and digital subtraction angiography. Radiology 219:108–113

92. Cottier JP, Bleuzen-Couthon A, Gallas S, Vinikoff-Sonier CB, Bertrand P, Domengie F, Barantin L, Herbreteau D (2003) Intracranial aneurysms treated with Guglielmi detachable coils: is contrast material necessary in the follow-up with 3D time-of-flight MR angiography? Am J Neuroradiol 24:1797–1803

93. Okahara M, Kiyosue H, Hori Y, Yamashita M, Nagatomi H, Mori H (2004) Three-dimensional time-of-flight MR angiography for evaluation of intracranial aneurysms after endosaccular packing with Guglielmi detachable coils: comparison with 3D digital subtraction angiography. Eur Radiol 14:1162–1168

94. Yamada N, Hayashi K, Murao K, Higashi M, Iihara K (2004) Time-of-flight MR angiography targeted to coiled intracranial aneurysms is more sensitive to residual flow than is digital subtraction angiography. Am J Neuroradiol 25:1154–1157

95. Hartman J, Nguyen T, Larsen D, Teitelbaum GP (1997) MR artifacts, heat production, and ferromagnetism of Guglielmi detachable coils. Am J Neuroradiol 18:497–501

96. Gonner F, Heid O, Remonda L, Nicoli G, Baumgartner RW, Godoy N, Schroth G (1998) MR angiography with ultra-short echo time in cerebral aneurysms treated with Guglielmi detachable coils. Am J Neuroradiol 19:1324–1328

97. Farb RI, Nag S, Scott JN, Willinsky RA, Marotta TR, Montanera WJ, Tomlinson G, Terbrugge KG (2005) Surveillance of intracranial aneurysms treated with detachable coils: a comparison of MRA techniques. Neuroradiology 47:507–515

98. Gauvrit JY, Leclerc X, Pernodet M, Lubicz B, Lejeune JP, Leys D, Pruvo JP (2005) Intracranial aneurysms treated with Guglielmi detachable coils: usefulness of 6-month imaging follow-up with contrast-enhanced MR angiography. Am J Neuroradiol 26:515–521

99. Lylyk P, Ceratto R, Hurvitz D, Basso A (1998) Treatment of a vertebral dissecting aneurysm with stents and coils: technical case report. Neurosurgery 43:385–388

100. Sekhon LH, Morgan MK, Sorby W, Grinnell V (1998) Combined endovascular stent implantation and endosaccular coil placement for the treatment of a wide-necked vertebral artery aneurysm: technical case report. Neurosurgery 43:380–383

101. Wakhloo AK, Lanzino G, Lieber BB, Hopkins LN (1998) Stents for intracranial aneurysms: the beginning of a new endovascular era? Neurosurgery 43:377–379

102. Phatouros CC, Sasaki TY, Higashida RT, Malek AM, Meyers PM, Dowd CF, Halbach VV (2000) Stent-supported coil embolization: the treatment of fusiform and wide-neck aneurysms and pseudoaneurysms. Neurosurgery 47:107–113

103. Brassel F, Rademaker J, Haupt C, Becker H (2001) Intravascular stent placement for a fusiform aneurysm of the posterior cerebral artery: case report. Eur Radiol 11:1250–1253

104. Fiorella D, Albuquerque FC, Han P, McDougall CG (2004) Preliminary experience using the Neuroform stent for the treatment of cerebral aneurysms. Neurosurgery 54:6–16

105. Wanke I, Doerfler A, Schoch B, Stolke D, Forsting M (2003) Treatment of wide-necked intracranial aneurysms with a self-expanding stent system: initial clinical experience. Am J Neuroradiol 24:1192–1199

106. Alfke K, Straube T, Dorner L, Mehdorn HM, Jansen O (2004) Treatment of intracranial broad-neck aneurysms with a new self-expanding stent and coil embolization. Am J Neuroradiol 25:584–591

107. Lubicz B, Piotin M, Mounayer C, Spelle L, Moret J (2005) Selective endovascular treatment of intracranial aneurysms with a liquid embolic: a single-center experience in 39 patients with 41 aneurysms. Am J Neuroradiol 26:885–893

108. Molyneux AJ, Cekirge S, Saatci I, Gal G (2004) Cerebral Aneurysm Multicenter European Onyx (CAMEO) trial: results of a prospective observational study in 20 European centers. Am J Neuroradiol 25:39–51

109. Lenhart M, Volk M, Manke C, Nitz WR, Strotzer M, Feuerbach S, Link J (2000) Stent appearance at contrast-enhanced MR angiography: in vitro examination with 14 stents. Radiology 217:173–178

110. Maintz D, Tombach B, Juergens KU, Weigel S, Heindel W, Fischbach R (2002) Revealing in-stent stenoses of the iliac arteries: comparison of multidetector CT with MR angiography and digital radiographic angiography in a Phantom model. Am J Roentgenol 179:1319–1322

111. Nehra A, Moran CJ, Cross DT, 3rd, Derdeyn CP (2004) MR safety and imaging of neuroform stents at 3T. Am J Neuroradiol 25:1476–1478

112. Saatci I, Cekirge HS, Ciceri EF, Mawad ME, Pamuk AG, Besim A (2003) CT and MR imaging findings and their implications in the follow-up of patients with intracranial aneurysms treated with endosaccular occlusion with onyx. Am J Neuroradiol 24:567–578